

## Structure of a corystosperm fossil forest from the Late Triassic of Argentina

Analía E. Artabe<sup>a,b,\*</sup>, Luis A. Spalletti<sup>c</sup>, Mariana Brea<sup>d</sup>, Ari Iglesias<sup>a,b</sup>,  
Eduardo M. Morel<sup>a,e</sup>, Daniel G. Ganuza<sup>a</sup>

<sup>a</sup> *División Paleobotánica, Facultad de Ciencias Naturales y Museo, Universidad Nacional de La Plata, Paseo del Bosque SN, 1900 La Plata, Argentina*

<sup>b</sup> *Consejo Nacional de Investigaciones Científicas y Técnicas (CONICET), Argentina*

<sup>c</sup> *Centro de Investigaciones Geológicas, Facultad de Ciencias Naturales y Museo, Universidad Nacional de La Plata y CONICET. Calle 1 nro 644, 1900 La Plata, Argentina*

<sup>d</sup> *Laboratorio de Paleobotánica, Centro de Investigaciones Científicas, Diamante (CICYTTP-CONICET), Argentina*

<sup>e</sup> *Comisión de Investigaciones Científicas de la Provincia de Buenos Aires, Argentina*

Received 12 September 2005; received in revised form 23 August 2006; accepted 28 August 2006

### Abstract

A palaeoecological study of a standing Late Triassic forest containing 150 silicified stumps from the Río Blanco Formation of Mendoza province, Argentina is described. A mapped portion of the forest floor provides quantitative data — tree density, mean separation of trees and basal area per stump — which, along with taxonomic and sedimentologic information, allowed the reconstruction of a plant community that grew along river banks and within proximal floodplain environments. Analysis of architectural and phenological data from monotypic forest indicates an evergreen community composed of a corystosperm genus with a canopy height of c. 13–21 m. The corystosperm taxon: *Elchaxylon*, like *Rhexoxylon*, has polyxylic axes with centripetal secondary xylem but does not generate perimedullar bundles and the centrifugal secondary xylem produces an undivided solid pycnoxylic cylinder. Vegetation analysis shows that the forest has a clustered distribution pattern with high density. Forest density ranges between 727 and 1504 trees/ha but there are first order clusters with elevated density (mean nearest neighbour distance of 1.85 m). The histogram of diameter classes based on 131 stumps suggests an earlier colonization by few older pioneers (the largest ones) followed by establishment of a large younger cohort of coeval trees. Based on 9 series and 139 rings, the mean ring width and mean sensitivity (MS) were 3.47 mm and 0.31 respectively. MS values and the presence of false rings indicate the forest community responded to stressed ecosystems. The growth rings are very erratic and range from 0.27 to 8.94 mm. For fossil growth analysis it was assumed that wider rings would suggest a warmer climate and the considerable range in growth rates would indicate variability in the limiting factors among subsequent cycles.

© 2006 Elsevier B.V. All rights reserved.

**Keywords:** Triassic; Argentina; Fossil forest; Tree rings; Fossil wood; Palaeoclimatology

\* Corresponding author. División Paleobotánica, Facultad de Ciencias Naturales y Museo, Universidad Nacional de La Plata, Paseo del Bosque SN, 1900 La Plata, Argentina.

E-mail addresses: [aartabe@museo.fcnym.unlp.edu.ar](mailto:aartabe@museo.fcnym.unlp.edu.ar) (A.E. Artabe), [spalle@cig.museo.unlp.edu.ar](mailto:spalle@cig.museo.unlp.edu.ar) (L.A. Spalletti), [cidmbrea@infoaire.com.ar](mailto:cidmbrea@infoaire.com.ar) (M. Brea), [aiglesias@museo.fcnym.unlp.edu.ar](mailto:aiglesias@museo.fcnym.unlp.edu.ar) (A. Iglesias), [emorel@museo.fcnym.unlp.edu.ar](mailto:emorel@museo.fcnym.unlp.edu.ar) (E.M. Morel), [dganuza@museo.fcnym.unlp.edu.ar](mailto:dganuza@museo.fcnym.unlp.edu.ar) (D.G. Ganuza).

## 1. Introduction

*In situ* petrified forests are very scarce in the geological record and their occurrences have contributed significantly to our understanding of past ecosystems. The Triassic fossil record of Argentina shows that the forested landscape was dominated by corystosperms and by coniferophytes. Corystosperms are interpreted to have constituted the largest emergent (uppermost) or canopy (second) stratum of the *in situ* mixed forests found in the Paramillo and Cortaderita Formations (Brea, 1995, 1997; Brea and Artabe, 1999; Spalletti et al., 1999; Brea, 2000; Artabe et al., 2001; Artabe and Brea, 2003). They also made up riparian monotypic forests in the Ischigualasto Formation (Zamuner, 1992). The three *in situ* petrified forests found in central west Argentina were assigned to the *Yabeiella mareyesiaca*, *Scytophyllum bonettiae*, *Protocircoporoxylon* (= *Protophyllocladoxylon*) *cortaderitaensis* Assemblage Biozone (MBC) (late Middle Triassic) and *Yabeiella brackebuschiana*, *Scytophyllum neuburgianum*, *Rhexoxylon piatnitzkyi* Assemblage Biozone (BNP) (early Late Triassic) assemblage biozones of the Cortaderitian Stage (Spalletti et al., 1999; Artabe et al., 2001; Morel et al., 2003). At very high latitudes, in the central Transantarctic Mountains, another *in situ* monotypic corystosperm riparian forest was found and assigned to the Middle Triassic (Cúneo et al., 2003).

The present study concentrates on an *in situ* corystosperm monotypic forest that occurred in the Río Blanco Formation at La Elcha Mine (Cuyo Basin). This unit was included in the *Dictyophyllum tenuiserratum*, *Linguifolium arctum*, *Protocircoporoxylon marianaensis* Assemblage Biozone (DLM) (Florian Stage, Late Triassic) (Spalletti et al., 1999). Although it is the first *in situ* preserved forest found in the Late Triassic of Argentina, corystosperm permineralized wood has been found in the uppermost Triassic sections of the Cuyo (Artabe et al., 1999) and the Ischigualasto–Villa Unión basins (Caminos et al., 1995).

The main purpose of the present contribution is to develop a reconstruction of La Elcha community based on quantitative forest information (mean separation of trees, density, and basal area per stump). Also, the spatial distribution pattern was integrated with the taxonomic-phenological data in order to infer the environmental conditions under which the community developed. Growth-ring analyses were used to determine tree habit and paleoclimatic conditions. Mean ring width, thinnest ring, widest ring, mean sensitivity (MS), annual sensitivity (AS), proportion of late wood to early wood, presence or absence of false rings and the cumulative sum of deviations from mean radial diameter were calculated and plotted as the CSDM curve.

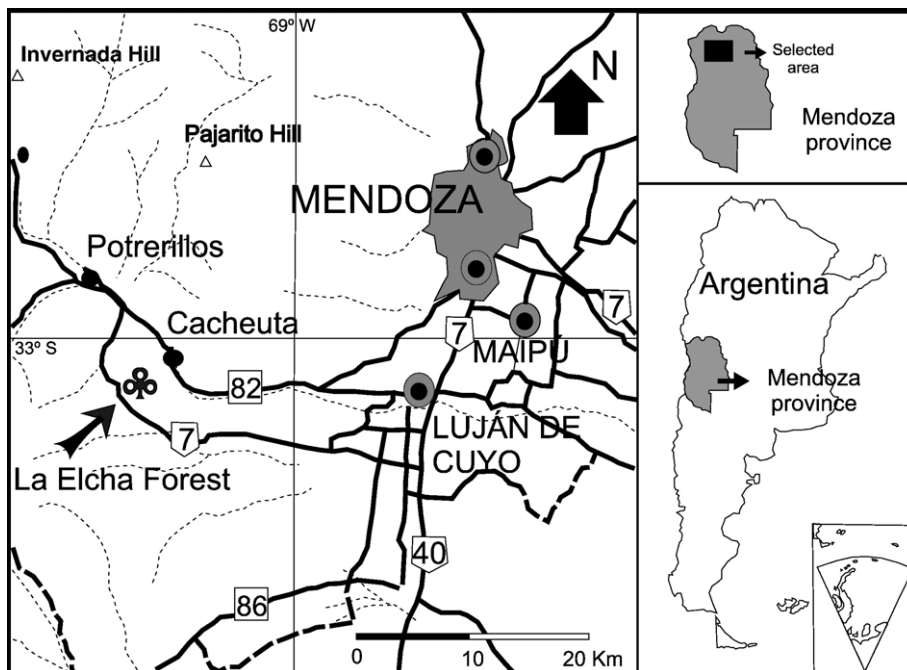


Fig. 1. Map showing La Elcha Mine locality, Mendoza province, Argentina, where the fossil forest was preserved.

**2. Materials and methods**

The fossil stumps described in this paper have been found in the lower levels of the Rio Blanco Formation at La Elcha Mine (near Cacheuta hill), situated in the southern Precordillera, Mendoza Province, western Argentina (69° 09' 24.3" W and 33° 03' 36.8" S; Fig. 1). Following

the palaeobotanical biozonation made by Spalletti et al. (1999) for the continental Triassic of Argentina, the taphocenosis is located in the upper Biozone of the Florian Stage (DLM Assemblage Biozone), which corresponds to the latest Triassic.

At the studied locality, the Río Blanco Formation was examined in detail and a vertical section of its lower part

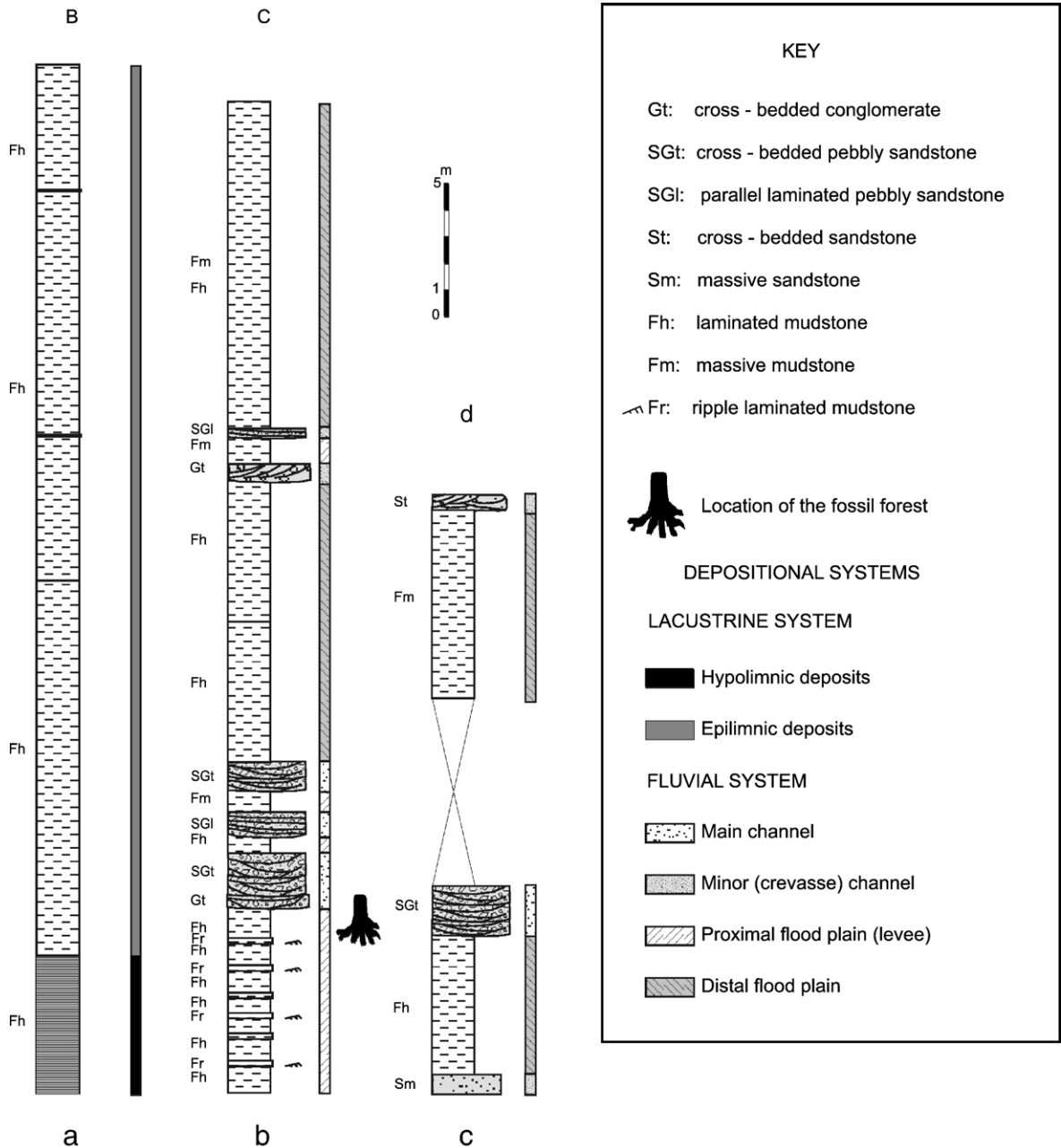


Fig. 2. Lithostratigraphic lower section of Rio Blanco Formation at La Elcha locality, showing the main facies associations and the position of the fossil forest level.

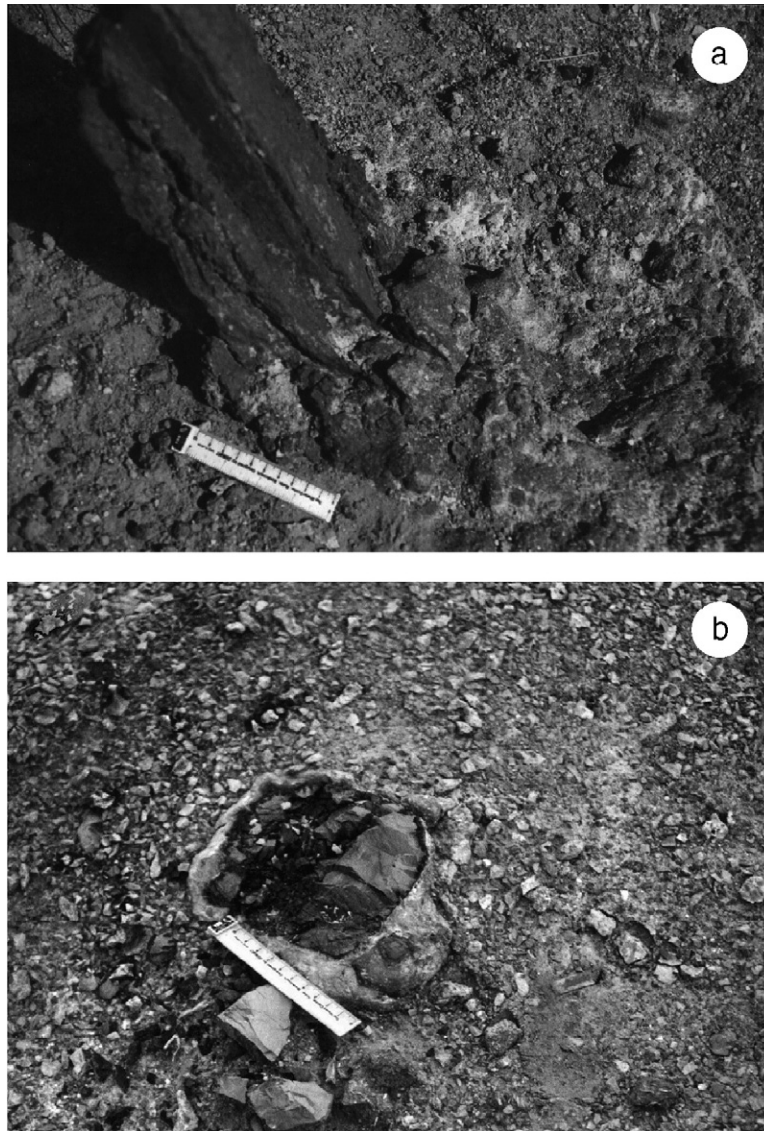


Fig. 3. General view of a medium-sized corystosperm stump in La Elcha locality. Scale: 10 cm.

was measured with bed-by-bed logging (Fig. 2). In this paper we summarize the key sedimentological features.

The forest has 150 stumps in life position (Fig. 3) that were mapped at 1:500 scale using a Brunton compass and tape measure. To analyse the two-dimensional distribution arrangements of the vegetation a spatial statistical package created to analyze crime incident location data was used. The *CrimeStat II* program (Ned Levine, 2002) provides a variety of tools to describe the overall spatial distribution, the dominant pattern of distribution and sub-regional patterns or 'neighbourhood' patterns within the overall distribution. The density of the *in situ* permineralized stumps was calculated using the distance to its nearest neighbour for each

stump as well as the mean distance of stumps in the study area. For identifying the degree of clustering of trees, the nearest neighbour index (Nni) was used because it provides an approximation about whether trees are more clustered or dispersed than would be expected on the basis of chance. To recognize groups of trees that are clustered together on the basis of spatial proximity the nearest neighbour hierarchical spatial clustering (Nnh) was used. To identify groups that are spatially close, the Nnh uses two criteria: the *threshold distance* (in La Elcha forest, the probability selected was 0.99) and the minimum number of trees (in La Elcha forest, six trees) to be included in each first order cluster.

Table 1

La Elcha fossil forest: coordinates  $x$  and  $y$  (in meters) of trees and diameters (in meters)

Tree number	$X$	$Y$	Diameter	Tree number	$X$	$Y$	Diameter	Tree number	$X$	$Y$	Diameter
1	308.44	8.46	0.18	51	204.95	183.76	0.21	101	42.87	394.55	0.15
2	313.82	13.52	0.24	52	206.37	186.24	0.3	102	43.35	402.67	0.25
3	313.82	20.24	0.5	53	194.16	189.71	0.23	103	46.75	408.38	0.19
4	308.07	25.50	0.39	54	194.66	190.81	0.23	104	50.26	408.66	0.24
5	306.74	25.62	0.27	55	189.99	195.37		105	34.02	399.72	0.2
6	303.85	34.84	0.48	56	193.73	194.12	0.32	106	51.64	391.52	0.23
7	271.38	92.27	0.3	57	193.88	196.60	0.4	107	54.59	389.94	0.2
8	251.23	110.40	0.35	58	184.60	208.87	0.46	108	52.45	404.87	0.3
9	246.27	113.76		59	187.51	209.82	0.23	109	37.53	405.79	0.2
10	242.05	112.19	0.27	60	185.10	210.25	0.36	110	40.76	415.20	0.17
11	245.63	125.28	0.26	61	185.70	214.02	0.17	111	38.54	428.29	
12	243.00	123.19	0.3	62	181.35	216.21	0.26	112	32.84	412.70	0.36
13	242.38	125.28	0.2	63	181.42	230.04	0.39	113	33.29	402.02	0.2
14	241.99	127.22	0.26	64	185.92	222.50		114	30.15	404.05	0.24
15	247.76	129.80	0.22	65	185.21	223.21		115	37.90	421.73	0.34
16	247.76	128.88	0.22	66	184.67	224.10		116	27.76	422.29	0.23
17	244.64	132.88	0.19	67	183.40	228.49		117	29.05	416.39	0.19
18	244.14	133.51	0.2	68	179.82	231.80	0.24	118	29.61	413.72	0.33
19	243.58	134.32	0.24	69	169.10	239.97	0.22	119	26.66	414.45	0.15
20	243.58	135.21	0.22	70	177.63	241.39		120	27.22	411.13	0.28
21	248.32	133.55	0.19	71	178.06	239.58	0.3	121	26.57	426.89	0.11
22	245.07	137.02	0.38	72	176.53	241.39		122	24.44	429.67	0.2
23	239.51	117.59	0.2	73	157.99	256.83	0.37	123	23.62	428.38	0.17
24	237.17	138.07	0.22	74	147.61	257.54	0.38	124	34.78	436.76	0.24
25	238.87	134.82		75	154.03	250.22	0.17	125	37.25	434.93	0.09
26	239.08	135.53		76	154.03	246.30	0.27	126	39.56	432.99	0.12
27	236.99	135.81		77	158.83	251.14	0.17	127	19.55	440.72	
28	236.67	142.14		78	150.52	255.49	0.075	128	25.37	439.34	0.34
29	237.21	143.41		79	114.47	295.99	0.18	129	17.61	438.70	0.14
30	237.77	144.64		80	98.47	334.32	0.26	130	23.99	443.02	0.17
31	230.66	149.48	0.16	81	84.17	353.38		131	31.18	441.65	
32	237.04	130.94	0.29	82	92.40	330.75	0.22	132	25.93	445.43	
33	241.45	123.32	0.27	83	91.56	328.42	0.25	133	27.48	449.57	0.12
34	227.65	155.25	0.37	84	93.11	334.56	0.21	134	19.83	449.94	0.19
35	228.04	157.86	0.28	85	87.86	335.01	0.28	135	19.47	451.23	0.11
36	224.12	156.87	0.26	86	97.29	325.06		136	29.61	452.97	
37	226.38	158.07		87	91.09	341.84	0.16	137	27.86	460.36	0.15
38	223.08	159.07	0.25	88	83.42	352.71	0.45	138	32.19	470.22	0.16
39	221.17	160.66	0.25	89	83.89	345.52	0.15	139	27.95	475.00	0.24
40	220.89	157.86	0.27	90	84.63	339.53		140	23.62	476.01	0.17
41	217.10	166.77	0.22	91	81.40	339.53	0.25	141	21.40	459.15	0.16
42	216.54	151.85	0.2	92	77.43	347.37	0.13	142	23.26	459.80	
43	219.23	151.46	0.05	93	74.12	351.79		143	21.12	481.83	0.21
44	216.00	168.82	0.3	94	76.61	353.64	0.21	144	24.07	484.97	0.26
45	215.33	170.37	0.23	95	80.21	355.30		145	21.77	484.69	0.17
46	218.13	168.26	0.3	96	67.40	367.72	0.21	146	19.10	491.49	0.2
47	214.51	175.71	0.37	97	73.30	369.94	0.31	147	17.53	490.22	0.58
48	213.46	181.78	0.26	98	64.99	388.29	0.27	148	14.21	522.20	0.2
49	205.28	177.97	0.3	99	50.34	388.29	0.12	149	6.40	525.32	0.16
50	206.09	182.11	0.34	100	42.33	391.15	0.11	150	23.62	521.92	0.14
										Tot	124

In the case of La Elcha forest, the stem basal diameter was also measured for each stump (Tables 1 and 2) and the total basal area was obtained by multiplying number of trees per ha by the mean basal area per ha (Cottam

and Curtis, 1956). Also, using the basal diameter of stumps, their critical buckling heights ( $H_{crit}$ ) were calculated using Niklas' formula (1994a,b):  $H_{crit} = C(E/\rho)^{1/3}D^{2/3}$ ; where  $C$  is a constant, 0.792;  $E$  represents

Table 2

La Elcha fossil forest: Coordinates  $x$  and  $y$  (in meters) of trees of area 1 and area 2

Area 1								
Tree number	$X$	$Y$	Tree number	$X$	$Y$	Tree number	$X$	$Y$
8	22.05	4.67	30	28.13	40.95	53	13.60	101.86
9	19.59	10.16	31	24.43	48.89	54	14.57	102.55
10	15.24	10.94	32	20.19	29.12	55	12.78	108.97
11	24.89	20.50	33	18.16	17.19	56	15.33	105.79
12	21.38	19.91	34	24.95	55.20	57	16.67	107.87
13	22.05	22.12	35	26.46	57.41	58	15.09	123.18
14	22.75	23.85	36	22.51	58.51	59	17.99	122.59
15	29.02	23.33	37	25.19	58.51	60	16.15	124.04
16	28.54	22.53	38	22.85	60.82	61	18.64	127.11
17	28.13	27.50	39	21.82	63.26	62	16.02	131.42
18	27.85	28.15	40	20.37	60.84	63	23.09	143.05
19	40.76	29.12	41	23.01	70.57	64	23.26	134.36
20	28.30	29.99	42	13.47	57.92	65	22.92	135.18
21	31.50	26.05	43	15.74	56.37	66	22.92	136.28
22	30.46	30.92	44	21.64	72.82	67	23.96	140.84
23	26.68	35.26	45	21.84	74.38	68	22.85	145.32
24	24.02	35.61	46	23.33	71.20	69	17.47	157.84
25	24.02	32.02	47	23.78	81.54	70	25.51	154.70
26	24.54	32.61	48	23.78	81.45	71	24.95	153.02
27	22.88	33.82	49	17.08	86.31	72	24.67	155.22
28	25.77	39.44	50	19.91	89.28	73	16.54	178.05
29	27.09	39.96	51	19.78	91.42	74	8.09	183.91
			52	22.23	92.58	75	9.77	174.16
						76	7.85	170.70
						77	14.40	172.71
						78	9.47	180.48
Área 2								
Tree number	$X$	$Y$	Tree number	$X$	$Y$	Tree number	$X$	$Y$
80	24.06	11.31	101	7.07	91.48	123	7.72	131.09
81	21.62	34.98	102	11.76	98.18	124	21.77	132.02
82	17.25	11.50	103	17.36	101.28	125	22.92	150.62
83	15.31	9.88	104	20.54	99.63	126	23.78	126.27
84	19.65	14.42	105	2.10	100.50	127	10.59	142.96
85	15.26	17.38	106	12.91	84.22	128	14.85	138.94
86	18.49	4.15	107	14.92	81.56	129	14.36	142.40
87	21.69	21.75	108	20.54	95.52	130	15.35	142.96
88	20.71	34.94	109	8.15	103.78	131	21.04	137.86
89	17.51	28.56	110	15.63	110.27	132	18.44	144.00
90	14.92	23.03	111	10.53	105.95	133	21.84	146.72
91	12.19	24.63	112	7.87	112.09	134	15.50	150.53
92	12.84	33.23	113	2.62	102.64	135	15.78	152.04
93	12.11	38.79	114	1.23	106.18	136	25.51	148.52
94	15.46	39.14	115	16.65	117.62	137	27.61	155.55
95	19.31	38.68	116	8.30	123.09	138	36.32	162.03
96	14.49	55.91	117	6.36	117.25	139	35.35	168.52
97	20.84	54.90	118	5.34	114.53	140	32.00	171.22
98	22.85	74.92	119	3.26	116.61	141	21.58	157.95
99	10.31	103.74	120	2.03	113.88	142	23.55	157.38
100	4.84	88.97	121	9.51	127.20	143	32.67	177.45
			122	9.02	131.03	144	36.95	178.75
						145	34.75	179.85
						146	36.09	187.07
						147	34.14	186.64

Table 3  
Sedimentary facies of the Río Blanco Formation at the studied locality

		Structure	Conglomerate	Pebbly sandstone	Sandstone	Mudstone
“Coarse member”	Main facies	Trough x-stratification Low-angle lamination	Gt Gl	SGt SGL	St	
	Subordinated facies	Parallel lamination Massive, clast-supported			Sm	Fh Fm
“Fine Member”	Main facies	Current ripples Parallel lamination				Fr Fh
		Massive, clast-supported			Sm	Fm
	Subordinated facies	Trough x-stratification Low-angle lamination	Gt l	SGt SGL	St	

Young’s modulus ( $958.1 \times 10^6 \text{ kg m}^{-2}$ );  $\rho$  is the wood density ( $468.9 \text{ kg m}^{-3}$ ); and  $D$  is the basal diameter (m). Thus, the critical buckling heights of fossil trees may be estimated. In practice, the calculation resolves into a multiplication of  $D^{2/3}$  by 95.75. The critical buckling height ( $H_{\text{crit}}$ ) is the height at which the mechanical structure of the wood fails, leading to the collapse of the tree. Because trees never attain  $H_{\text{crit}}$ , estimated tree heights were calculated on the basis of trunk diameter to height ratios observed in living trees ( $H_{\text{est}} = 27.8 \text{ d}^{0.430}$  Niklas, 1993, 1994a,b) using known stump diameters. The Safety Factor (SF) was obtained dividing the  $H_{\text{crit}}$  by the actual estimated height ( $H_{\text{est}}$ ). Using SF a more accurate estimated high ( $H_{\text{est}}$ ) for La Elcha fossil wood was obtained.

The growth rings of the corystosperm genus were quantitatively analyzed. Using the method described by Falcon-Lang (2000a): the radial diameters of successive tracheid cells were measured across each growth increment. Five adjacent files of cells were measured for each ring increment and these data were averaged to give the final plots. Using these data, the cumulative algebraic sum of each cell’s deviation from the mean of the radial diameters was calculated for each growth ring increment and plotted as a zero-trending curve (CSDM curve). For each ring increment the percentage skew of the zenith of CSDM curves with respect to the centre of the plot was calculated.

Taking into account that deciduous conifers give CSDM curves which are dominantly left-skewed or symmetrical while evergreen conifers have dominantly right-skewed CSDM curves, the new genus habit was inferred. Because the percentage of latewood may be strongly influenced by leaf longevity in addition to reflecting intensity of climate seasonality, two aspects of growth ring were quantified using the Falcon-Lang technique (2000b) to calculate the Ring Markedness Index (RMI). The percentage of diminution in a ring increment was considered using the percentage of diminution ( $x$ ) =  $(b/a) 100$ ; where  $a$  = maximum cell

diameter and  $b$  = maximum cell diameter minus minimum cell diameter. The percentage of latewood in each growth ring increment was calculated using Creber and Chaloner’s method (1984): Percentage of latewood ( $y$ ) =  $(d/c) 100$ ; where  $d$  = number of cells in each ring increment,  $c$  = number of cells after the CSDM curve turns to zero for the last time. The product of these two parameters was calculated to give a Ring Markedness Index (RMI) (=  $x \cdot y$ ).

Growth ring analysis has the main purpose of relating ring growth patterns to palaeoclimate (Creber, 1977; Creber and Chaloner, 1984). The growth ring sequences were measured in well-preserved trunks and two parameters, mean growth-ring width and Mean Sensitivity (MS) were calculated. The latter is a quantitative measure of the year to year variability in ring width within specimen and is defined by the formula:

$$\text{MS} = \frac{1}{N-1} \sum_{t=1}^{N-1} \left| \frac{2(X_{t+1} - X_t)}{(X_{t+1} + X_t)} \right|$$

where  $x$  is ring width,  $n$  the number of rings in the sequence analyzed, and  $t$  is the year number of each ring (Fritts, 1976). MS values can range from zero, where there is no year to year variability, to a maximum approaching to representing the greatest possible variability. High MS values are considered diagnostic of growth under stressful environmental conditions (Creber and Francis, 1999). Sensitive ring sequences formed under variable, stressful conditions have MS values above 0.3 while complacent ring sequences formed under uniform, favorable conditions have MS values below 0.3 (Fritts, 1976). In order to obtain growth ring width expressed in millimeters, an ESSEX electronic digital gauge was used, with a 0.01 mm accuracy.

### 3. Geological setting

Triassic basins located along the proto-Pacific margin of Gondwana (western South America) are narrow and

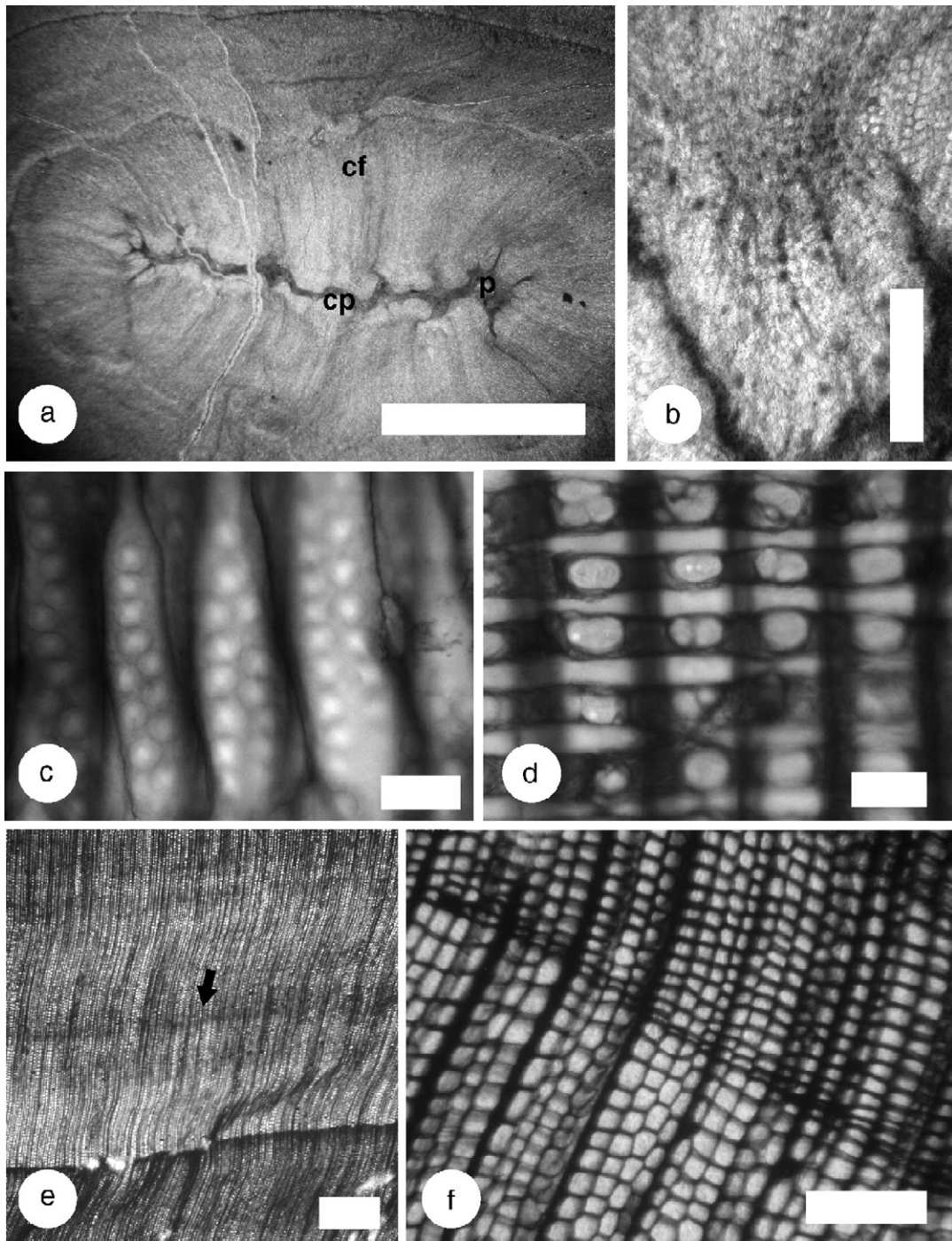


Fig. 4. *Elchaxylon zavattieriae*. a, transverse section showing the central part of the stem: (p) pith, (cp) centripetal secondary xylem, (cf) centrifugal secondary xylem. b, detail of a, centripetal secondary xylem showing tracheids of mesarch protoxylem. c, tracheids in radial section showing uni-biseriate radial pitting. d, radial section of wood showing ray with simple pits in the cross fields. e, transversal section of wood showing a false ring. f, transversal section of wood showing a growth ring. (bar-scales A: 5 mm; B: 500  $\mu$ m; C, D: 25  $\mu$ m; E: 250  $\mu$ m; F: 500  $\mu$ m).

elongated depressions oriented NW–SE, floored by a thick continental crust composed of Precambrian and Lower Palaeozoic magmatic rocks, and an Upper

Palaeozoic plutonic–volcanic complex. These passive rift systems formed as a result of a generalised extension and are infilled by continental volcanoclastic and



Table 4  
Nearest neighbour analysis based on a sample size of 150 trees and the outcrop area of 34,357 m<sup>2</sup>

Mean nearest neighbour distance	Expected nearest neighbour distance	Nearest neighbour index	Test statistic (Z)
3.7868	7.5561	0.50115	-11.6881

pyroclastic deposits associated with lava flows and plutonic intrusions. The causes of extension along the proto-Pacific margin of Gondwana are linked to the tectonic activity of the margin (Franzese and Spalletti, 2001). Lithospheric thickening related to Upper Paleozoic convergence caused a strong gravitational instability in the orogenic belt between 30° and 40° S. Subsequent cessation of subduction during the Late Permian to Early Jurassic caused the collapse of the subducted slab and the generation of an asthenosphere window. As a result, anomalous heating of the upper mantle produced bimodal magmatism, uplift, thermal weakening and gravitational collapse of the upper crust (Franzese and Spalletti, 2001).

The Cuyo Basin is a 30,000 km<sup>2</sup> elongated basin located in western Argentina between 32° and 36° South Latitude (Fig. 1). It is the most important hydrocarbon-producing Triassic basin of western Gondwana. The total thickness of Triassic sediments is over 3500 m, and its terrigenous clastic record reflects successive episodes of continental deposition. The stratigraphic succession of the basin is shown in Fig. 2. Two megasequences bounded by regional unconformities have been recognised (Kokogian and Mancilla, 1989; Kokogian et al., 1993). The first one is restricted to the central parts of the basin and is composed of proximal fluvial deposits. The upper megasequence is widely distributed and is

characterised by fluvial, deltaic and lacustrine depositional systems.

The Río Blanco Formation was formed during the latest post-rift phase of evolution of the Cuyo Basin. It is composed of a 230 m thick red bed succession of mudstones, sandstones, pebbly sandstones and conglomerates. These deposits have been previously described by Lluch (1971), Strelkov and Álvarez (1984), Kokogian and Boggetti (1986), Frey and Rosenfeld (1991), Spalletti et al. (1995) and Spalletti and Barrio (1998). All these authors interpreted the Río Blanco Formation as deposited in holomictic lakes, deltaic and high sinuosity fluvial systems.

#### 4. The Río Blanco Formation at La Elcha Mine. Sedimentology

The outcrops at La Elcha Mine record the lowermost section of the Río Blanco Formation. These deposits conformably overlie the lacustrine black shales of the Cacheuta Formation and are composed of two main facies associations, commonly referred to as “fine member” and “coarse member” (Allen, 1965) (Table 3). Towards the base of the section, the Río Blanco Formation is composed of a thick package (34 m) of yellowish, greenish and purple mudstones and clays-tones with very thin intercalations of fine-grained pyroclastic fall out deposits. These deposits are followed by thinner (0.5–12 m thick) and laterally extensive mudstone and heterolithic intervals, which are interstratified with sandstone, pebbly sandstone, and fine-grained conglomerate beds (“coarse member”). The heterolithic deposits are characterised by alternations of massive mudstones and thin cross-laminated fine-grained sandstone and siltstone layers (Fig. 2). The

Table 5  
Nearest Neighbour Hierarchical Clustering analysis based on 150 sample size (likelihood of grouping pair of points by chance: 0.99000 (99.000%); Z-value for confidence interval: 2.326)

Order	Cluster	Mean X	Mean Y	Rotation	X-axis	Y-axis	Area	Points	Density
1	1	242.82609	128.73913	77.44489	12.91541	5.25771	213.33125	23	0.107814
1	2	29.10000	428.95000	80.45895	16.44126	8.75541	452.23206	20	0.044225
1	3	43.57143	400.57143	48.99544	13.53135	9.71488	412.97922	14	0.033900
1	4	217.85714	164.71429	65.72984	15.42478	4.91646	238.24346	14	0.058763
1	5	85.2666	343.00000	54.77362	15.99172	5.21323	261.90974	15	0.057272
1	6	24.00000	454.71429	26.89529	6.44622	7.57745	153.45387	7	0.045616
1	7	180.75000	229.33333	66.81451	15.51028	4.29123	209.09859	12	0.057389
1	8	200.00000	187.83333	35.60246	11.99574	2.34925	88.53311	6	0.067771
1	9	23.50000	481.75000	59.06442	13.23820	2.43241	101.16168	8	0.079081
1	10	154.00000	252.83333	54.57405	8.00543	5.68593	143.00000	6	0.04195
2	1	41.08762	421.79714	64.83485	96.08611	12.72079	3839.94136	5	0.001302
2	2	199.08665	192.69068	55.62788	98.13508	5.50742	1697.94092	5	0.002945



Fig. 5. A detailed (1:500) map of fossil stumps was prepared using Brunton compass and tape measure. To recognize groups of trees that are clustered together on the basis of spatial proximity, the nearest neighbour hierarchical spatial clustering (Nnh) was used. Two orders of clustering were recognized. The trees are grouped into 10 first order groups which, in turn, are grouped into two second order groups. There are five first order groups in each second order group.

gravelly and sandy deposits commonly constitute less than 2 m thick multistorey, lenticular but laterally extensive bodies. They are uniform from bottom to top

as well as laterally, and are formed by trough cross-bedded multilateral sets. Sets range from 0.5 to 0.8 m thick and their boundaries are generally concave up and

horizontal with respect to depositional dip. Conglomerate layers with horizontal and/or low-angle cross-bedding occur sporadically. The clast population in conglomerates is dominated by ignimbritic and rhyolitic clasts, and grain shapes range from subangular to rounded.

Based on sand body geometry, facies composition and scale, three architectural elements (Miall, 1985, 1988) are recognised in the studied area: lake deposits (LD), overbank fines (OF) and channels (CH).

The lake element is composed of the yellowish, greenish and purple mudstones and claystones located at the base of the Río Blanco Formation. These fine-grained deposits are finely laminated and even fissile. Slickensides are common. It is likely that these deposits represent the infilling of a hydrologically open lake. The scarcity of burrows and the abundance of laminae combined with light colours would reflect rapid sediment accumulation rather than anoxic conditions (cf. Aslan and Autin, 1999). Frequent intercalation of fine-grained ash layers indicates coeval explosive volcanism.

Overbank fines consist primarily of red massive and/or fissile mudstones characterised by a sheet-like geometry which encase sand bodies of varying sizes and shapes. The fine-grained texture, root traces and mottles, and small iron nodules suggest a well drained backswamp environment (Coleman, 1966; Aslan and Autin, 1999). Heterolithic intervals composed of alternating massive mudstones and ripple laminated or

Table 6  
Distance analysis based on sample one (68 trees and bounding area of 6533.90 m<sup>2</sup>) and sample two (71 trees and bounding area of 5898.79 m<sup>2</sup>)

	Sample size	Mean nearest neighbour distance (m)	Expected nearest neighbour distance	Nearest neighbour index	Test statistic (Z)
Snd Order Group One	71	2.58	4.56	0.5653	-7.0070
Group 1	22	2.67	2.95 m	0.7573	-0.8653
Group 4	14	1.85	2.1958 m	0.84382	-1.1179
Group 8	7	2.32	2.5355 m	0.9162	-0.4237
Group 7	12	2.22	2.5413 m	0.8762	-0.8202
Group 10	6	4.23	2.2079 m	1.91818	4.3026
Snd order Group Two	68	3.71	4.90	0.7573	-3.8281
Group 5	16	4.82	2.8504 m	1.69170	5.2931
Group 3	14	3.84	3.4898 m	1.10175	0.7283
Group 2	20	4.26	3.5178 m	1.20993	1.7960
Group 9	8	3.06	2.2913 m	1.33874	1.8329
Group 6	8	3.29	1.9764 m	1.66714	3.6099

Table 7

Tree densities of modern conifer mixed forest growing in Argentina and Chile

Kind of forest	Associated species	Density	Source
Mixed <i>Fitzroya cupressoides</i> forest	Associated with <i>Nothofagus betuloides</i> .	660–4400 trees/ha	Donoso, 1993
Mixed <i>Fitzroya cupressoides</i> forest	Associated with <i>Nothofagus nitida</i> .	1227–4134 trees/ha	Donoso, 1993
Mixed <i>Fitzroya cupressoides</i> forest	Associated with other evergreen species ( <i>Gevuina avellana</i> , <i>Podocarpus nubigena</i> , <i>Saxegothaea conspicua</i> , <i>Laurelia philippiana</i> , etc).	600.780 tees/ha	Donoso, 1993
Mixed <i>Austrocedrus chilensis</i> forest		460 trees/ha	Donoso, 1993
Mixed <i>Araucaria araucana</i> forest	Associated with evergreen species like: <i>Austrocedrus chilensis</i> , <i>Nothofagus pumilio</i> , <i>N. Antarctica</i> , <i>Saxegothaea conspicua</i> , etc.	1059–1125 trees/ha	Donoso, 1993

massive fine-grained sandstones and siltstones are up to 7 m thick and can be traced over more than 500 m laterally. They represent levee deposits developed near channel margins (Hughes and Lewin, 1982; Diemer and Belt, 1991). Mudstones contain abundant soil features; they are bioturbated, mottled, and show subangular blocky structure locally. The *in situ* corystosperm forest described in this paper was developed on these soils. Sheet sand and gravel bodies 0.20 to 0.95 m thick are encased within fine-grained overbank deposits. They have sharp and erosional lower boundaries and can be traced laterally for up to 100 m. The characteristics of these coarse-grained bodies indicate that these deposits represent small crevasse channel fills.

Channels comprise dominantly fine-to medium-grained conglomerates with subordinate pebbly sandstones. These sediments are moderately sorted and dominantly subangular to rounded. Channels are characterized by a convex upwards lens shape or sheet like cross section. They are 1 to 2 m thick and tens to hundreds of meters wide. They have a typical shoestring geometry. The basal erosion surfaces underlying the channel bodies have local relief of several decimeters. Storeys are almost entirely composed of trough cross-bedded multilateral sets. Most of them are 30–65 cm thick. These bedforms are explained as gravel dunes migrating downstream. CH elements represent fixed channels that show no signs of lateral migration. The

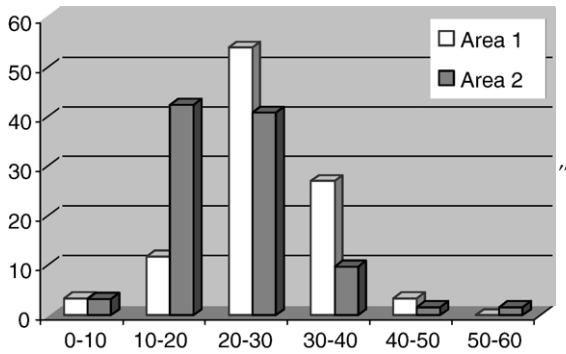


Fig. 6. The histogram of diameter classes based on 131 stumps developed a normal curve with a tail in largest values.

encasement of the channels within fine-grained over-bank deposits and the sharp upper boundaries suggest that relocation of the channel belts was produced by abrupt avulsion (Rhee et al., 1993).

In comparison with the classic conceptual models, the fluvial system of the Río Blanco Formation at La Elcha Mine described here shows more frequent downstream accreting 3D gravelly macroforms. Fluvial channels are shoestring-shaped and comparatively small. The sharp vertical transition from channel facies to fine-grained flood plain facies suggests avulsive processes for channel abandonment.

The sedimentary record of the studied section shows the evolution from a hydrologically open lacustrine system to a mixed-load fluvial system. La Elcha forest was developed during the early stages of accumulation of the Río Blanco fluvial system, and the trees colonized well-drained proximal flood-plain areas, close to channel belts.

## 5. Systematic paleobotany

The permineralized stumps found at La Elcha Mine (Río Blanco Formation, Late Triassic) were recently described and assigned to Corystospermaceae: *Elchaxylon zavattieriae* Artabe and Zamuner (in press).

All trunks have been examined in the field with a 15X hand lens and it was corroborated that they have the same anatomical structure and taphonomic tissue preservation. To check the systematic assignment 30 specimens randomly sampled were sectioned. The collected samples were placed at Museo de La Plata Palaeobotanical Collection. The trees — fossilized in growth position — were decorticated during the preservation process; therefore, the cortex zone is not preserved (Fig. 4a). The stems are oval-circular. The polyxylic gymnospermous axes have two discontinuous cambial

rings, which develop centrifugal secondary xylem and centripetal secondary xylem around the mesarch primary xylem bundles (Fig. 4a, b). The centrifugal undivided pycnoxylic secondary xylem shows uniseriate rays, uni-biseriate radial pitting either alternate or opposite and 1–2 simple pits in cross field (Fig. 4c, d). The secondary xylem shows growth rings and false rings (Fig. 4e, f).

The pycnoxylic wood associated with a unique mode of secondary xylem production, which results in polyxylic stems, relates *Elchaxylon* to *Rhexoxylon* Bancroft *emend.* Archangelsky and Brett, 1961 and also to the Corystospermaceae (Artabe and Zamuner, in press). *Elchaxylon* is considered a polyxylic stem because the stem possesses two discontinuous cambial rings, which start developing centrifugal secondary xylem and centripetal secondary xylem around the mesarch primary xylem bundles. As *Rhexoxylon*, the new genus is characterized by: mesarch primary xylem, centrifugal secondary xylem, centripetal secondary xylem (inverted xylem); however, it does not develop perimedullar bundles or centripetal polyxyly (Zamuner, 1992; Artabe et al., 1999; Artabe and Brea, 2003). *Rhexoxylon* — like the other southwestern Gondwanaland genus assigned to Corystospermaceae: *Cuneumxylon* Artabe and Brea, 2003 and *Tranquiloxyton* Herbst and Lutz, 1995 — has two kinds of unusual centrifugal secondary growth (Artabe and Brea, 2003). The first one shows unequal activity of different portions of the cambium on the circumference of the axes; consequently, the reduction of cambial activity to certain restricted areas develops wedged stems, which often split. The second type of unusual secondary growth is the appearance of secondary xylem with included phloem producing centrifugal polyxylic stems (Artabe and Brea, 2003). Wood characters also relate *Elchaxylon* to *Rhexoxylon*. In this sense, they have uni-triseriate radial pitting and cross fields with 1–4 simple pits and secondary rays mainly uniseriate. It seems clear that *Elchaxylon* shows anomalous secondary growth like *Rhexoxylon*, *Cuneumxylon* and *Tranquiloxyton*. The presence of centripetal secondary xylem could have

Table 8  
Structural data of La Elcha forest

	Area 1	Area 2
Mean distance to neighbour	2.58 m	3.71 m
Mean diameter of trees	0.27 m	0.24 m
Mean area	6.65 m <sup>2</sup>	13.76 m <sup>2</sup>
Mean height of trees	14.77 m	14.24 m
Density (trees/ha)	1503	726
Mean basal area per ha	0.057 m <sup>2</sup> /ha	0.045 m <sup>2</sup> /ha
Total basal area (total forest cover/ha)	85.6 m <sup>2</sup> /ha	32.67 m <sup>2</sup> /ha

Table 9

Basal diameters of trunks were used to calculate the critical buckling heights ( $H_{crit}$ ), the estimated height ( $H_{est}$ ) and the Safety Factor (2.466) and a second estimated height using Niklas (1993, 1994a,b) method

		$N$		$H_{crit}$	$H_{est(1)}$	$H_{est(2)}$
Area 1	59	Minimum diameter	0.05 m	13.00	7.67	5.27
		Maximum diameter	0.50 m	60.32	20.63	15.00
		Mean diameter	0.27 m	40.00	15.83	16.22
Area 2	61	Minimum diameter	0.075 m	17.03	9.13	6.90
		Maximum diameter	0.58 m	66.83	21.99	27.00
		Mean diameter	0.21 m	33.83	14.21	13.72
Total area	120	Minimum diameter	0.05 m	13.25	7.66	5.27
		Maximum diameter	0.58 m	66.59	21.99	27.00
		Mean diameter	0.24 m	36.98	15.05	15.00

important phylogenetic implications. It was suggested that the corystosperm stele evolved along two principal lineages (rhexoxyloid and cuneumxyloid) from a medullosan or a similar precursor (Artabe and Brea, 2003). *Rhexoxylon* characterizes the rhexoxyloid line and shows: mesarch primary xylem, centrifugal wedges of secondary xylem, centripetal secondary xylem (inverted xylem) and perimedullar bundles. The southwestern Gondwanaland species seem to fit into a developmental series: *R. sp.-R. krauselii* ?-(Lutz and Herbst, 1992), *R. piatnitzkyi* Archangelsky and Brett, 1961 and *R. brunoi* Artabe et al., 1999. The series shows an increase of the anomalous vascular tissue development with formation of successive cycles of medullar bundles inside the trunk and the progressive acquisition of bigger stems by an increase in the amount of centrifugal secondary conducting tissues. *Elchaxylon* could represent a branch of rhexoxyloid line. This branch initiates in the first stage of the rhexoxyloid line, represented by *Rhexoxylon* sp. (*R. krauselii*). *Elchaxylon*, like this last species, has centripetal secondary xylem but does not produce perimedullar bundles and

like in the rhexoxyloid line, *Elchaxylon* shows an increment of pycnoxyly.

## 6. Vegetation analysis

The fossil forest architectural analysis embraces three main aspects: 1. taxonomic composition, 2. horizontal structure, referring to the spatial distribution of trees, and 3. vertical distribution, indicating canopy position.

1. The taxonomic study allows La Elcha to be characterized as a monotypic forest. Pure forests constituted by only one species are usually considered a result of a restrictive edaphic or climatic condition in extant ecosystems (Donoso, 1993). Edaphic and climatic restrictions are the most important factors in the development of Southwestern Chile–Argentina pure conifer forests (*Austrocedrus chilensis*, *Fitzroya cupressoides* and *Araucaria araucana* forests; Donoso, 1993). Monotypic forest are also made up by pioneer species which colonized areas affected by natural catastrophic events — such as volcanic eruptions and sudden water overflows — that devastated the former forest (Donoso, 1993).

2. To analyse the spatial distribution of vegetation, a statistical package (Crimestat program) was used. Based on the total sample size of 150 stumps (Table 1), the nearest neighbour analysis provides the following data: a mean nearest neighbour distance of 3.79 m and a total density of 696.37 trees/ha (Table 4). The total forest area, selected as sample unit, produces two distortions on the density estimation. First, the density misrepresentation is related to the vegetation distribution pattern. The total density could be considered as a representative value when the distribution pattern is random or homogeneous, meanwhile whether points are more clustered or dispersed than would be expected on the basis of chance, they do not constitute an accurate measure. Second, the total forest area includes scarcely preserved sectors that should not be considered. To solve both problems, the nearest neighbour index (Nni) and the nearest neighbour hierarchical spatial clustering (Nnh) were used. The Nni

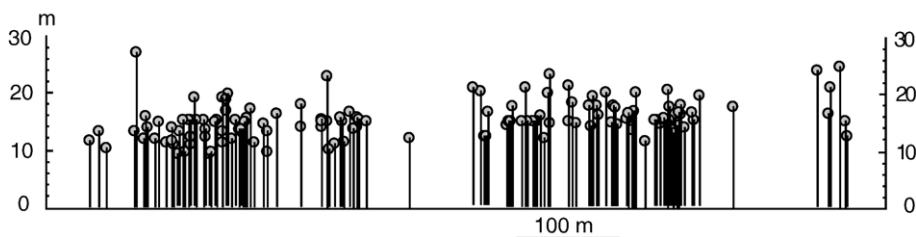


Fig. 7. Lateral view of La Elcha forest showing the deduced height of the trees, based on the stumps diameter.

Table 10

Results of the quantification of ring markedness parameters and percentage of skew of CSDM curves (Falcon-Lang, 2000a,b) for the measured *Elchaxylon zavattierae*

	Percentage of diminution	Percentage of latewood	Ring Markedness Index	Percentage of skew
Ring 1	70.00	30.43	7.58	+24.63
Ring 2	66.19	26.15	21.30	+13.84
Ring 3	70.26	32.81	17.31	+12.5
Ring 4	73.09	41.17	23.05	+20.58
Mean	69.88	32.64	30.09	+17.89

allows the identification of the presence of tree clustering. It compares the average distance of the nearest other point (nearest neighbour) with a spatially random expected distance by dividing the empirical average nearest neighbour distance by the expected random distance. The result data (Table 4) indicate that the trees are grouped (Nni=0.50).

To recognize groups of trees clustered together on the basis of spatial proximity, Nnh was used. Two orders of clustering were recognized. The trees are grouped into 10 first order groups which, in turn, are grouped into two second order groups. There are five first order groups in each second order group (Table 5, Fig. 5). The two second order clusters outlined the better preserved regions and dismissed the trees which appear more isolated, including geographical sectors affected by recent erosion processes. So, the linkages between the small clusters of first order to the bigger second order clusters allow recognizing the two selective areas of taphonomic importance.

According to the above data, two new sample data sets were selected (Table 2) and new distance analyses were made (Table 6). Taking into account the mean nearest neighbour distance for each area (2.58 and 3.71 m), the density ranges between 726.74 and 1503.75 tree/ha respectively (Table 6). The closely space distribution found in second order groups may imply that this vegetation was a continuous forest, while the strongly high first order density (Mean Nearest Neighbor Distance of first order clusters ranges between 1.85–4.82 m) shows a low intraspecific competition among the taxon considered. Although the stand density in modern conifer forest varies widely and is a result of factors such as the particular population dynamics of the community, site disturbance regime, and stand age (Donoso, 1993; Pole, 1999), mixed forests generally show higher density values than pure forests growing under restrictive conditions. As shown in Table 7, La Elcha forest has tree densities similar to many extant

mid-latitude mixed forests (Donoso, 1993). Also, the tree density of La Elcha forest (726.74 and 1503.75 tree/ha) is bigger than other Triassic forests of Gondwana (Brea, 1995; Cúneo et al., 2003; Brea et al., 2005) offering a different distribution pattern as well. The monotypic forest found in the Middle Triassic of Antarctica (Cúneo et al., 2003) shows low density: 274.12 trees/ha, while the *in situ* Middle Triassic mixed forest found at the Paramillo Formation in Agua de la Zorra, northwestern Cuyo Basin, Argentina, the density ranges 600–700 trees/ha and the distribution pattern is homogeneous (Brea et al., 2005).

The clustered distribution of extant plant is a common feature of different kinds of vegetation. According to Donoso (1993), there are three causal factors related with clustered distribution. First, the kind of seeds and dispersion forms could generate clustered distribution. In general, the bigger and heavier seeds will fall and concentrate near the parent trees, forming seedling clustering which result in clustered trees. Secondly, the vegetative propagated species often produce aggregated forests by means like sending out runners (stolons). Lastly, differences among forest environments could produce the aggregate distribution pattern (Donoso, 1993). Some of these aspects described for corystosperms (Petriella, 1985; Zamuner, 1992) could be the main causes of the clustered distribution pattern in La Elcha forest. Also, the clustered and close space distribution restricted the foliage developed and permits inferring a palm-like habit. Assuming *Rhexoxylon* as the stem of the *Dicroidium*, an accurate plant reconstruction has been made, suggesting “*Dicroidium*” was probably a tree with a palm-like general appearance of trees with a crown of leaves at the top of the stem (Petriella, 1978).

The histogram of diameter classes based on 131 stumps developed a normal curve with a tail in largest values (Fig. 6). 46.56% of basal diameter trees measure 20–30 cm; 27.48%, between 10–20 cm; and 19.08%, among 30–40 cm. In summary, the results show that 93.1% of basal diameter trees range between 10–40 cm. Based on the configuration of the histogram of class diameters (Fig. 6), it is clear that there are a few older trees with diameters above 40 cm (4.59% of the stand) and a large younger cohort of trees with smaller diameters (93.1% of the stand). This suggests an earlier colonization by a few pioneers (the largest ones) followed by the establishment of a large number of coeval trees. The low number of individuals with diameters less than 10 cm (2.29%) indicates a low rate of breeding. Besides, it is interesting to remark that the groups of area 1 presented a more clustered pattern, though they are conformed by bigger trees.

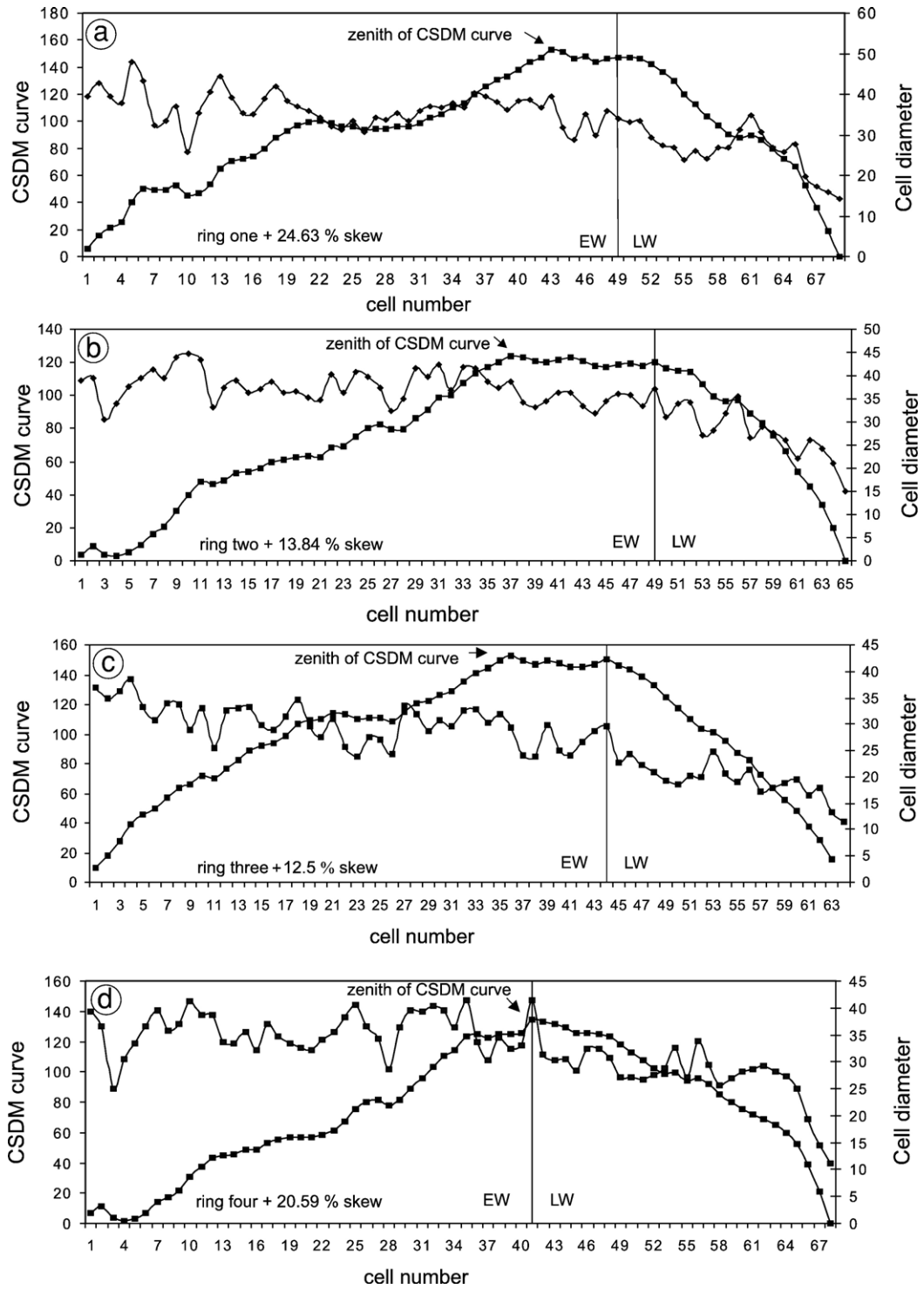


Fig. 8. Right-skewed CSDM curves of four growth rings and cell diameters of growth ring increment ( $\mu\text{m}$ ). For each ring increment the percentage of skew for CSDM curves was calculated using Falcon-Lang method (2000a). The distance where CSDM curve reaches the zenith represents the percentage of skew in relation with the total distance between the centre of the CSDM curve to the right of the plot.

Table 11

The growth ring analysis: mean growth ring width, minimum ring width, maximum ring width, Mean Sensitivity (MS) and Annual Sensitivity (AS), presence of false rings, was carried out on 9 series of grows rings, for a total of 140 rings

Specimen number (pm LBBP)	Number of rings	Mean ring-width (mm)	Minimum ring-width	Maximum ring-width	Mean sensitivity	AS		Presence of false rings
						Minimum value	Maximum value	
1740	21	1.39	0.44	4.75	0.35	0.0105	1.0351	Yes
1741	24	1.43	0.27	5.04	0.49	0.0208	1.0260	Yes
1746	23	2.38	1.02	3.72	0.38	0.0076	1.0599	Yes
1747	35	0.91	0.33	1.93	0.34	0.0080	0.9705	Yes
1750	5	4.99	2.79	7.45	0.46	0.3136	0.6423	Yes
1751	4	5.10	4.29	6.98	0.22	0.1932	0.2570	Yes
1754	5	5.21	4.52	6.72	0.10	0.0177	0.2702	Yes
1757	6	7.26	5.25	8.94	0.13	0.0704	0.2529	Yes
1758	17	2.52	0.98	3.9	0.31	0.0155	0.8121	Yes
Average	140	3.46	0.27	8.94	0.31	0.0730	0.7028	

In additional, the total basal area was calculated. In La Elcha forest, it ranges from 32.67 m<sup>2</sup>/ha in area 2 to 85.6 m<sup>2</sup>/ha in area 1 (Table 8). In extant forests, it commonly ranges between 20–50 m<sup>2</sup>/ha. The monotypic corystosperm forest found in the Middle Triassic of Antarctica (Cúneo et al., 2003) shows values of 20.83 m<sup>2</sup>/ha whereas in the mixed Triassic forest of Argentina this parameter has not been studied yet.

3. To analyse the vertical distribution of vegetation, the basal diameters of trunks were used to estimate the critical buckling heights ( $H_{crit}$ ), the estimated height ( $H_{est}$ ) and the

Safety Factor (Niklas, 1993, 1994a,b). Taking into account this factor, a second value of estimated heights was calculated to *Elchaxylon* trees (Table 9).

*Elchaxylon zavattieriae* has an average estimated tree height of 15 m when living. According to Niklas (1993, 1994a,b) a maximum height of 27 m corresponds to a stump diameter of 0.58 m, while the minimum measured diameter of 0.05 m would have represented an individual up to 5.27 m tall. As stature is the major factor controlling canopy position, the deduced height of *Elchaxylon* (considering the distribution of class

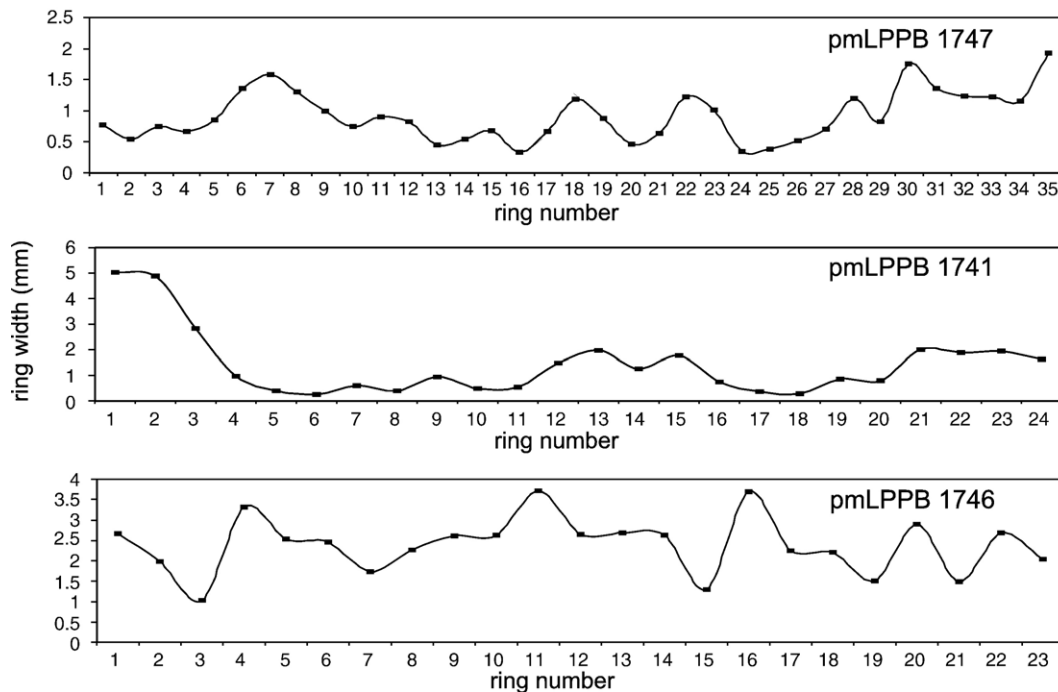


Fig. 9. Plots of three largest growth ring sequences showing the variable growth from year to year. Data from Table 11.





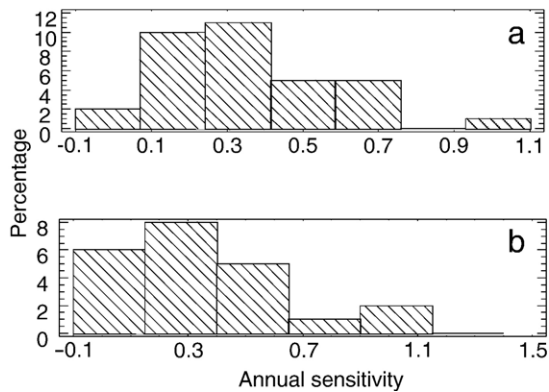


Fig. 10. Histograms showing the amount of annual variation in the growth patterns of selected fossil trees. a, specimen LPPB 1747; b, specimen LPPB 1746.

States indicate strong seasonality (Dubiel et al., 1991; Parrish, 1993; Dubiel and Smoot, 1994; Dubiel, 1994). In fact, on the basis of Falcon-Lang's interpretation, the subtle growth rings of the Chinle trees would be the result of long LRTs. Also, it is interesting to note that these 'growth rings' do not reflect annual growth periods but formed following growth interruptions related with drought of irregular duration and frequency (Falcon-Lang, 2000b). Thus, the irregular growth rings of *Elchaxylon* with a broad percentage of latewood could probably record a monsoonal climate.

Growth ring sequences were measured as well and the mean growth ring width, MS and AS were studied. Growth ring analysis was carried out on 9 series of growth rings, for a total of 140 rings (Table 11; Fig. 9). The mean ring width is 3.46 mm; growth rings widths are very erratic and range in different specimens from 0.27 to 8.94 mm. For fossil growth analysis, it was assumed that wider rings suggest a warmer climate (Fritts, 1976) and the considerable range in growth rates would indicate variability in the limiting factors among subsequent cycles. Like other Triassic woods of the Parana Basin, Brazil, the common occurrence of false growth rings within the early wood of many rings might suggest intermittent droughts during the growing season (Pires et al., 2005). The mean MS is 0.31 and ranges between 0.10 and 0.49. The more representative series show MS values greater than 0.3, which correspond to sensitive types (Fritts, 1976; Francis, 1984; Creber and Francis, 1999). AS values show great thickness rings variations from 1 year to the next, showing strong seasonality (Table 11; Fig. 10). The variable width of the rings, the common presence of false rings together with high MS values also may indicate that the forest community inhabited stressful niches.

## 8. Conclusions

1. The *in situ* corystosperm monotypic forest occurs in one fossiliferous stratum located in the lower part of the Río Blanco Formation at La Elcha Mine (Cuyo Basin). This unit was included in the DLM Assemblage Biozone (Floriant Stage, Late Triassic). 150 stumps in life position were preserved in an area 550 m long and 340 m wide.

2. The permineralized stumps found at La Elcha Mine were recently described and assigned to a new Corystospermaceae: *Elchaxylon zavattieriae* Artabe and Zamuner (in press). The polyxylic gymnospermous axes have two discontinuous cambial rings, which develop centrifugal secondary xylem and centripetal secondary xylem around the mesarch primary xylem bundles. The centrifugal undivided pycnoxylic secondary xylem shows uniseriate rays, uni-biseriate radial pitting either alternate or opposite and 1–2 simple pits in cross-field. The pycnoxylic wood associated with a unique mode of secondary xylem production, which results in polyxylic stems, relates *Elchaxylon* to *Rhexoxylon* and also to the Corystospermaceae.

3. The vegetation analysis shows that the forest has a clustered distribution pattern. The forest density ranges between 727–1504 trees/ha but there are first order clusters with mean nearest neighbour distance of 1.85 m. The high density of first order clusters indicates a low intraspecific competition among the taxon. The closely-spaced stem distribution probably restricted lateral foliage development and resulted in a palm-like general appearance of trees with a crown of leaves at the top of the stem.

4. The configuration of the histogram of class diameters suggests an earlier colonization made by few older pioneers (the largest ones) followed by establishment of a large younger cohort of coeval trees.

The height of the new corystosperm trees was predicted. Using Niklas' equations, estimated tree heights were calculated. Corystosperm wood fossils have a mean stem diameter ( $D$ ) of 24 cm (5–58 cm), with a mean estimated height ( $H_{est}$ ) of 15 m (5–27 m). As stature is the major factor controlling canopy position, the deduced height of *Elchaxylon* (considering the distribution of class diameters) suggests that the canopy in the forest community would have the majority of individuals ranging 13.27–21.07 m. A palm-like habit was inferred for *Elchaxylon zavattieriae*.

5. The quantitative growth ring anatomy analysis method described by Falcon-Lang was used to conjecture that the trees had been evergreen gymnosperms. The cumulative algebraic sum of each cell deviation from the

means was calculated for each growth ring increment and plotted as a zero-trending curve (CSDM curve). Like the evergreen conifers, the new corystosperm genus possesses right-skewed CSDM curves.

6. Based on 9 series and 139 rings, the mean ring width and mean sensitive (MS) were 3.17 mm and 0.31 respectively. MS values and the presence of false rings may indicate the forest community colonized stressed ecosystems.

## Acknowledgements

We would like to thank the financial support provided by the Consejo Nacional de Investigaciones Científicas y Técnicas (Project PIP 2148) and the Agencia Nacional de Promoción Científica y Tecnológica (PICT 07-08467). The authors want to express their acknowledgement to Ana María Zavattieri and Augusto Menéndez who gave us the first sample of the trees and the references to locate the fossil forest; to Marcelo Arturi, for his critical reading of the manuscript and to Amanda Zamuner, for correcting the English version.

## References

- Allen, J.R.L., 1965. Fining upward cycles in alluvial successions. *Geol. J.* 4, 229–246.
- Archangelsky, S., Brett, D., 1961. Studies on Triassic fossil plants from Argentina. 1. *Rhexoxylon* from the Ischigualasto formation. *Philos. Trans. R. Soc. Lond., B* 706 (244), 1–19.
- Artabe, A.E., Brea, M., 2003. A new approach to corystospermales based on petrified stems from the Triassic of Argentina. *Alcheringa* 27, 209–229.
- Artabe, A.E., Zamuner, A.B., in press. *Elchaxylon*, a new corystosperm based on permineralized stems of the Late Triassic of Argentina. *Alcheringa*.
- Artabe, A.E., Brea, M., Zamuner, A.B., 1999. *Rhexoxylon brunoi* Artabe, Brea et Zamuner, nov. sp., a new Triassic Corystosperm from the Paramillo de Uspallata, Mendoza, Argentina. *Rev. Palaeobot. Palynol.* 105, 63–74.
- Artabe, A.E., Morel, E.M., Spalletti, L.A., 2001. Paleoeología de las de las floras triásicas argentinas. In: Artabe, A.E., Morel, E.M., Zamuner, A.E. (Eds.), *El Sistema Triásico en la Argentina*. Fundación Museo de La Plata “Francisco P. Moreno”, La Plata, pp. 199–225.
- Ash, J., 1983. Growth ring in *Agathis robusta* and *Araucaria cunninghamii* from tropical Australia. *Aust. J. Bot.* 31, 269–275.
- Ash, J., 1985. Growth rings and longevity of *Agathis vitiensis* (Seeman) Benth. And Hook. F. ex Drake in Fiji. *Aust. J. Bot.* 33, 81–88.
- Ash, J., 1986. Growth rings, age and taxonomy of *Dacrydium* (Podocarpaceae) in Fiji. *Aust. J. Bot.* 34, 197–205.
- Ash, S., Creber, G.T., 1992. Palaeoclimatic interpretations of the wood structures of trees in the Chinle Formation (Upper Triassic), Petrified Forest National Park, Arizona, USA. *Palaeogeogr. Palaeoclimatol. Palaeoecol.* 96, 299–317.
- Aslan, A., Autin, W.J., 1999. Evolution of the Holocene Mississippi River floodplain, Ferriday, Louisiana: insights on the origin of fine-grained floodplain. *J. Sediment. Res.* 69, 800–815.
- Brea, M., 1995. Estudio de la paleoflora de la secuencia triásica de Agua de la Zorra, provincia de Mendoza. PhD Thesis N° 642, Fac. Cs. Nat. Mus., UNLP, Argentina, pp. 1–202.
- Brea, M., 1997. Una nueva especie fósil del género *Araucarioxylon* Kraus 1870 *emend.* Maheshwari 1972 del Triásico de Agua de la Zorra, Uspallata, Mendoza, Argentina. *Ameghiniana* 34, 485–496.
- Brea, M., 2000. Paleoflora triásica de Agua de la Zorra, Uspallata, provincia de Mendoza, Argentina: Lycophyta y Filicophyta. *Ameghiniana* 37 (2), 199–204.
- Brea, M., Artabe, A.E., 1999. Apocalamitaceae (Sphenophyta) triásicas de la Formación Paramillo, Agua de la Zorra, provincia de Mendoza, Argentina. *Ameghiniana* 36 (4), 389–400.
- Brea, M., Artabe, A.E., Spalletti, L.A., 2005. Paleovegetation studies and growth-ring analysis of a mixed Middle Triassic forest from Argentina. *Abstracts Gondwana* 12, 77.
- Caminos, R., Zamuner, A., Limarino, C., Fauqué, L., 1995. Hallazgo de Triásico superior en la Precordillera riojana. *Rev. Asoc. Geol. Argent.* 50 (1–4), 262–265.
- Coleman, J.M., 1966. Ecological changes in a massive fresh-water clay sequence. *Gulf Coast Assoc. Geol. Soc. Trans.* 16, 159–174.
- Cottam, G., Curtis, J.T., 1956. The use of distance measures in phytosociological sampling. *Ecology* 37, 451–460.
- Cúneo, N.R., Taylor, E.L., Taylor, T.N., Kring, M., 2003. *In situ* fossil forest from the upper Fremouw Formation (Triassic) of Antarctica: paleoenvironmental setting and paleoclimate analysis. *Palaeogeogr. Palaeoclimatol. Palaeoecol.* 197, 239–261.
- Chabot, B.F., Hicks, D.J., 1982. The ecology of leaf life spans. *Ann. Rev. Ecol. Syst.* 13, 229–259.
- Creber, G.T., 1977. Tree-rings: a natural data storage system. *Biol. Rev.* 52, 349–383.
- Creber, G.T., Chaloner, W.G., 1984. Influence of environmental factors on the wood structure of living and fossil trees. *Bot. Rev.* 50, 357–448.
- Creber, G.T., Francis, J.E., 1999. Tree ring analysis: palaeodendrochronology. In: Jones, T., Rowe, N. (Eds.), *Fossil Plants and Spores: Modern Techniques*. Geological Society of London Special Publication, pp. 245–250.
- Diemer, J.A., Belt, E.S., 1991. Sedimentology and paleohydraulics of the meandering river system of the Fort Union Formation, southeastern Montana. *Sediment. Geol.* 75, 85–108.
- Donoso, C., 1993. Bosques templados de Chile y Argentina. Variación, Estructura y Dinámica. *Ecología Forestal*. Editorial Universitaria, Santiago de Chile. 484 pp.
- Dubiel, R.F., 1994. Triassic deposystems, paleogeography, and paleoclimate of the Western Interior. In: Caputo, M., Peterson, J., Franczyk, K. (Eds.), *Mesozoic Systems of the Rocky Mountain Region*. U.S. Geological Survey, Denver, USA, pp. 133–168.
- Dubiel, R.F., Smoot, J.P., 1994. Criteria for interpreting paleoclimate from red beds — a tool for Pangaeon reconstructions. *Can. Soc. Pet. Geol., Mem.* 17, 295–310.
- Dubiel, R.F., Parrish, J.T., Parrish, J.M., Good, S.C., 1991. The Pagaean megamonsoon — evidence from the Upper Triassic Chinle Formation, Colorado Plateau. *PALAIOS* 6, 347–370.
- Fahn, A., 1990. *Plant Anatomy*. Pergamon Press. 588 pp.
- Falcon-Lang, H.J., 2000a. A method to distinguish between woods produced by evergreen and deciduous coniferopsids on the basis of growth ring anatomy: a new palaeoecological tool. *Palaeontology* 43 (4), 785–793.
- Falcon-Lang, H.J., 2000b. The relationship between leaf longevity and growth ring markedness in modern conifer woods and its implications for palaeoclimatic studies. *Palaeogeogr. Palaeoclimatol. Palaeoecol.* 160, 317–328.

- Franzese, J.E., Spalletti, L.A., 2001. Late Triassic–Early Jurassic continental extension in southwestern Gondwana: tectonic segmentation and pre-break-up rifting. *J. S. Am. Earth Sci.* 14, 257–270.
- Francis, J.E., 1984. The seasonal environment of the Purbeck (Upper Jurassic) fossil forest. *Palaeogeogr. Palaeoclimatol. Palaeoecol.* 48, 285–307.
- Frey, J.W., Rosenfeld, U., 1991. The strata of Potrerillos (Prov. of Mendoza/Argentina): a regionally typical profile of the continental Triassic in southern South America. *Zbl. Geol. Paläont. Teil. 1 (H.6)*, 1615–1632 (Stuttgart).
- Fritts, H.C., 1976. *Tree Rings and Climate*. Academic Press, London. 567 pp.
- Herbst, R., Lutz, A.I., 1995. *Tranquiloxydon petriellai* nov. gen. et sp. (Pteridospermales) from the Upper Triassic Laguna Colorada Formation, Santa Cruz province, Argentina. *Ameghiniana* 32, 231–236.
- Hughes, D.A., Lewin, J., 1982. Small scale flood plain. *Sedimentology* 29, 891–895.
- Kiddler, D.L., Worsley, T.R., 2004. Causes and consequences of extreme Permo-Triassic warming to globally equable climate and relation to the Permo-Triassic extinction and recovery. *Palaeogeogr. Palaeoclimatol. Palaeoecol.* 203, 207–237.
- Kokogíán, D.A., Boggetti, D.A., 1986. Estratigrafía y ambientes sedimentarios de los depósitos triásicos de la localidad de Potrerillos en la provincia de Mendoza. *Res. Exp. Reunión Arg. Sedimen., La Plata*, vol. 1, pp. 161–164.
- Kokogíán, D., Mancilla, O., 1989. Análisis estratigráfico y secuencial de la Cuenca Cuyana. In: Chebli, G., Spalletti, L. (Eds.), *Cuencas Sedimentarias Argentinas. Serie Correlación Geológica*, vol. 6. Universidad Nacional de Tucumán, pp. 169–201.
- Kokogíán, D., Fernández Seveso, F., Mosquera, A., 1993. Las secuencias sedimentarias triásicas. In: Ramos, V.A. (Ed.), *Relatorio Geología y Recursos Naturales de Mendoza. 12 Cong. Geol. Arg. y 2 Cong. Expl. Hidroc., Actas*, vol. 1 (7), pp. 65–78.
- Lluch, J., 1971. Sedimentología del Triásico en el área Papagallos-Divisadero Largo. Provincia de Mendoza. *Rev. Asoc. Argent. Mineral. Petrol. Sedimentol.* 2, 93–116.
- Looy, C.V., Brugman, W.A., Dilcher, D.L., Visscher, H., 1999. The delayed resurgence of equatorial forest after the Permian–Triassic crisis. *PNAS* 96, 13857–13862.
- Looy, C.V., Twitchett, R.J., Dilcher, D.L., Van Konijnenburg-van Cittert, J.H.A., Visscher, H., 2001. Life in the end-Permian dead zone. *PNAS* 98 (14), 7879–7883.
- Lutz, A.I., Herbst, R., 1992. Una nueva especie de *Rhexoxylon* del Triásico de Barreal, San Juan, Argentina. 7° Simp. Arg. Paleob. Palinol. (Corrientes 1991). *Publ. Espec. Asoc. Paleontol. Argent.* 2, 73–76.
- Miall, A.J., 1985. Architectural-element analysis: a new method of facies analysis applied to fluvial deposits. *Earth-Sci. Rev.* 22, 261–308.
- Miall, A.J., 1988. Reservoir heterogeneities in fluvial sandstones. Lessons from outcrop studies. *Bull. Am. Assoc. Pet. Geol.* 72, 682–697.
- Morel, E.M., Artabe, A.E., Spalletti, L.A., 2003. The Triassic floras of Argentina: Biostratigraphy, Floristic events and comparison with other areas of Gondwana and Laurasia. *Alcheringa* 27, 231–243.
- Ned Levine, CrimeStat II: A Spatial Statistics Program for the Analysis of Crime Incident Locations. Ned Levine and Associates, Houston, TX, and the National Institute of Justice, Washington, DC. May 2002.
- Niklas, K.J., 1993. The scaling of plant height: a comparison among major plant clades and anatomical grades. *Ann. Bot.* 72, 165–172.
- Niklas, K.J., 1994a. The allometry of safety-factors for plant height. *Am. J. Bot.* 81 (3), 345–351.
- Niklas, K.J., 1994b. Predicting the height of fossil plant remains: an allometric approach to an old problem. *Am. J. Bot.* 81 (10), 1235–1242.
- Parrish, J.T., 1993. Climate of the supercontinent Pangea. *J. Geol.* 101, 215–233.
- Petriella, B., 1978. La reconstrucción de *Dicroidium* (Pteridospermopsida, *Corystospermaceae*). *Obra del Centenario del Museo La Plata*, vol. 5, pp. 107–110.
- Petriella, B., 1985. Caracteres adaptativos y autoecología de las *Corystospermaceae*. 3° Congreso Latinoamericano de Paleontología (Mexico, 1984). *Simposio Floras Triásico, Mem.*, pp. 53–57.
- Pires, E.F., Guerra Sommer, M., dos Santos, C.M., 2005. Late Triassic Climate in southernmost Parana Basin (Brazil): evidence from dendrochronological data. *J. S. Am. Earth Sci.* 18, 213–221.
- Pole, M., 1999. Structure of a near-polar latitude forest from the New Zealand Jurassic. *Palaeogeogr. Palaeoclimatol. Palaeoecol.* 147, 121–139.
- Rhee, C.W., Ryang, W.H., Chough, S.K., 1993. Contrasting development patterns of crevasse channel deposits in Cretaceous alluvial successions, Korea. *Sediment. Geol.* 85, 401–410.
- Retallack, G.J., 1997. Earliest Triassic origin of *Isoetes* and quillwort evolutionary radiation. *J. Paleontol.* 71, 500–521.
- Spalletti, L.A., Barrio, C.A., 1998. Arquitectura y secuencias de los sistemas fluviales triásicos (Formación Río Blanco) en la Cuenca Cuyana, Argentina. *Rev. Asoc. Geol. Argent.* 53, 388–400.
- Spalletti, L.A., Artabe, A.E., Brea, M., Ganuza, D.G., 1995. Ambientes de acumulación y paleoflora en capas rojas triásicas de la Cuenca Cuyana, Mendoza. *Rev. Asoc. Geol. Argent.* 50, 175–188.
- Spalletti, L.A., Artabe, A.E., Morel, E.M., Brea, M., 1999. Biozonación paleoflorística y cronoestratigrafía del Triásico Argentino. *Ameghiniana* 36 (4), 419–451.
- Spalletti, L.A., Artabe, A.E., Morel, E.M., 2003. Geological factors and evolution of Southwestern Gondwana Triassic Plants. *Gondwana Res.* 6, 119–134.
- Strelkov, E.E., Álvarez, L.A., 1984. Análisis estratigráfico y evolutivo de la Cuenca Triásica Mendocina–Sanjuanina. *Cong. Geol. Arg.*, No. 9, Actas, vol. 3, pp. 115–130.
- Zamuner, A.B., 1992. *Estudio de una tafoflora de la localidad tipo de la Formación Ischigualasto (Neotrias)*, Provincia de San Juan. PhD Thesis N° 583, Fac. Cs. Nat. Mus., UNLP, Argentina, pp. 1–97.